# Turning a Hyperthermostable Metallo-Oxidase into a Laccase by Directed Evolution

Vânia Brissos,[†] Maura Ferreira,[†] Gregor Grass,[‡] and Lígia O. Martins*[,†]

[†]Instituto de Tecnologia Química e Biológica António Xavier, Universidade Nova de Lisboa, Av da República, 2780-157 Oeiras, Portugal

[‡]Bundeswehr Institute of Microbiology, DZIF, Partner Site of German Center for Infection Research, Neuherbergstrasse 11, Munich DE 80937, Germany

S *Supporting Information*
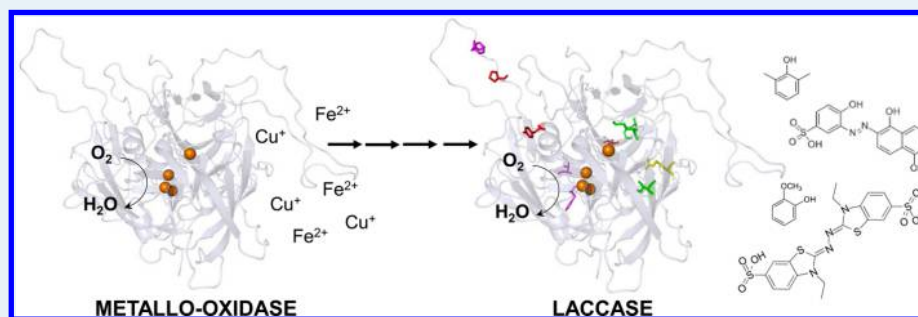
ABSTRACT: Multicopper oxidases are multifunctional enzymes that can be broadly divided into two functional classes: metallo-oxidases (with a robust activity toward metals, such as Cu^+ or Fe^{2+}) and laccases (with a superior catalytic efficiency for organic compounds). Laccases are green catalysts with an outstanding redox capability over a wide range of aromatic substrates using O_2 as an electron acceptor and releasing water as reduced product. Hyperthermostable laccases are highly in demand for their robustness in biotechnological applications. In this study, a laboratory evolution approach was conducted to improve the specificity of the metallo-oxidase McoA from the hyperthermophilic bacterium *Aquifex aeolicus* for aromatic compounds. Four rounds of random mutagenesis of the *mcoA*-gene followed by high-throughput screening (~94 000 clones) led to the identification of the 2B3 variant featuring a 2-order of magnitude higher catalytic efficiency (k_{cat}/K_m) than the wild-type enzyme for the typical laccase substrate ABTS (2,2′-azinobis(3-ethyl-benzothiazoline-6-sulfonic acid)) and additionally displaying a higher activity for phenolics and synthetic aromatic dyes. Notably, the recombinant 2B3 variant, unlike the wild-type, did not show temperature-dependent aggregation, exhibiting enhanced solubility and thus higher kinetic and thermodynamic thermostability. The structural basis of the altered substrate's catalytic efficiency and increased solubility/thermostability of the 2B3 variant are discussed on the basis of the biochemical analysis of single and double mutations of wild-type and its variants. The hyper-robustness of the evolved enzyme reported here shows clear advantages for current applications and provides a powerful tool for generation of more efficient biocatalysts for specific applications because it is widely acknowledged that thermostable proteins have an enhanced mutational robustness and evolvability.

KEYWORDS: *hyperthermophiles, enzyme specificity, protein aggregation, protein stability, ligninolytic enzymes, biorefineries*

INTRODUCTION

Laccases are enzymes belonging to the large family of multicopper oxidases (MCOs) that are encoded in the genomes of organisms in all three Domains of Life — Archaea, Bacteria, and Eukarya. MCOs couple the oxidation of four molecules of one-electron donor substrate with the reduction of one molecule of dioxygen to H_2O. These enzymes are distinguished by having three distinct copper sites, Cu types 1, 2, and 3; the oxidation of the reducing substrate occurs at the T1 Cu site, whereas the reduction of O_2 occurs at the T2/T3 trinuclear cluster.[1,2] The substrate specificity of MCOs is quite broad, and these enzymes are able to oxidize organic and inorganic substrates with varied specificity. One striking characteristic is the activity that only some MCOs, the so-called metallo-oxidases, exhibit toward metal ions, such as Cu(I) and Fe(II) as reducing substrate.[3] Laccases, because of their wide range of aromatic substrates and lack of requirement for exogenous cofactors, have found application in a large number of biotechnological applications in several industrial fields.[4,5] Additionally, laccases are the most promising ligninolytic enzymes, and therefore, it is expected that the number of laccase-based oxidation processes will increase significantly in the next few years in the lignocellulose biorefinery field, which represents a promising alternative source of renewable chemicals, materials, energy, and fuels.

In recent years, we have focused our attention on the study and application of prokaryotic members of MCOs:[6] the CotA-laccase from *Bacillus subtilis*[7−10] and the metallo-oxidases, McoC from *Campylobacter jejunii*,[11] McoA from the hyperthermophilic bacterium *Aquifex aeolicus*,[12] and McoP from the archaeon *Pyrobaculum aerophilum*.[13] McoA from *A. aeolicus*, which is encoded within a copper resistance operon in the genome of this bacterium, shows a notable thermoactivity (T_{opt} = 75 °C) and thermostability (temperature values at the midpoint (T_m) of 105, 110, and 114 °C) and a remarkable specificity constant (k_{cat}/K_m, also called catalytic efficiency) for the oxidation of cuprous and ferrous ions.[12,14] Therefore, the enzyme was designated a metallo-oxidase similar to CueO from *E. coli*[15] or Fet3p from yeast.[16] In the present study, we set up a directed evolution approach in order to increase the McoA's catalytic efficiency for aromatic compounds because enzymes, from extremophiles and thermophiles, in particular, are promising for industrial applications due to their robustness required for specific industrial processes.[6,17]

Directed laboratory evolution is a powerful protein engineering tool to tailor biocatalysts with improved features or new functions. By mimicking the principles of natural selection through iterative rounds of random mutagenesis and/or DNA recombination and screening, the time scale of evolution can be shortened to an experiment which can be conducted in the laboratory.[18−20] One of the major technologies underlying synthetic biology is the use of directed evolution for creating novel biocatalysts aiming at the synthesis of chemicals or degradation of toxic pollutants able to replace current polluting processes based on petrochemical feedstocks, organic solvents and heavy metal catalysts.[21−23] Novel enzymes, able to perform stereospecific and stereoselective reactions using both natural and synthetic products, are also a keystone in the pharmaceutical industry.[24,25] Over the last years, several directed evolution studies were performed in order to adapt laccases from mesophilic microorganisms to desired industrial demands such as to improved functional heterologous expression, activity for selected substrates, thermostability, and superior performance in non-natural conditions.[26−32]

In the present study, we describe the laboratory evolution of a hyperthermostable metallo-oxidase from the multicopper oxidase family into a laccase. An evolved variant was selected on the basis of increased 2,2′-azinobis(3-ethyl-benzothiazoline-6-sulfonic acid (ABTS) catalytic efficiency; the purified 2B3 variant showed a 100-fold increase in the oxidation rates of ABTS, 10-fold higher than that for Cu(I) oxidation, reaching activity levels similar to well-studied laccases. Importantly, the evolved enzyme features higher thermostability than that observed for the wild-type enzyme, which is mostly related to an increased resistance to temperature-induced aggregation. Analysis of single and double site-directed mutants and hit variants from each generation of *in vitro* evolution, guided the identification and discussion of the structure−function relationships that correlate the altered substrate specificity and improved solubility/thermostability of 2B3 hit variant.

■ MATERIALS AND METHODS

Bacterial Strains, Plasmids, and Media. *E. coli* strain DH5α (Novagen) was used for routine propagation and amplification of plasmid constructs. *E. coli* Tuner (DE3, Novagen) and KRX (Promega) strains in which the *cueO* gene, which codes for the multicopper oxidase CueO,[33] are inactivated (*E. coli* Tuner Δ*cueO*::*kan*, KRX Δ*cueO*::*kan*) were constructed by generalized phage P1*vir* transduction of a Δ*cueO*::*kan* cassette from strain W3110 replacing the *cueO* gene as described in ref 34. *E. coli* Tuner Δ*cueO*::*kan* or KRX Δ*cueO*::*kan* were used to express the *mcoA* gene previously cloned in pET-21a (+) plasmid (Novagen) or its evolved mutant variants. In the Tuner strain, the *mcoA* gene is under the control of T7 promotor, and its expression is induced by isopropyl *β*-D-1-thiogalactopyranoside (IPTG), whereas in the KRX strain, *mcoA* expression is under the control of the *rhaP*$_{BAD}$ promoter, induced by rhamnose. Luria−Bertani medium (LB) or Terrific Broth medium (TB) were used for the maintenance and growth of *E. coli* strains, supplemented with appropriate antibiotics when required.

Random Mutagenesis by Error-Prone PCR and Mutant Library Construction. Random variations in the *mcoA* gene were introduced by ep-PCR. Primers 5′-CCACTAAAGG-AGGTAACATATGGACAGGC-3′ (mcoA-182D) and 5′-GACTTGAATTCTCAACATATTGCACC-3′ (mcoA-1816R) were used for amplification (nucleotides for restriction sites of *Nde*I and *Eco*RI are underlined). ep-PCR was performed in a 50 μL final volume containing 3 ng of DNA template (plasmid pATF1,[14] containing the *mcoA* gene or its evolved variant genes), 1 μM of primers, 200 μM of dNTPs, 1.5 mM MgCl$_2$, *Taq* polymerase buffer, and 2.5 U of *Taq* polymerase (Fermentas). The effect of MnCl$_2$ was tested at 0.1−0.25 mM concentrations. After an initial denaturation period of 5 min at 94 °C, the following steps were repeated for 25 cycles in a thermal cycler (MyCycler thermocycler, Biorad): 1 min at 94 °C, 2 min at 55 °C, and 2 min at 72 °C followed by a final 10 min period at 72 °C. The amplified products were purified using GFX PCR DNA and Gel Band Purification kit (GE Healthcare). The final PCR products were digested with *Nde*I/*Eco*RI (Fermentas) and cloned into plasmid pET-21a (+) (Novagen). These pET-21a (+) plasmids expressing wild-type *mcoA* or its evolved variants were transformed into electrocompetent *E. coli* Tuner Δ*cueO*::*kan* cells.

Construction of *mcoA* Variants Using Site-Directed Mutagenesis. Single amino acid substitutions in the *mcoA* gene were created using the Quick change mutagenesis protocol developed by Stratagene. Plasmids containing the *mcoA* gene[14] and genes coding for different McoA variants were used as templates with appropriated primers (Table S1). PCRs were carried out in 50 μL reaction volumes containing 3 ng of DNA template, 2 μM of primers, 200 μM of dNTPs, NZYProof polymerase buffer, and 1.25 U of NZYProof polymerase (NZYTech). After an initial denaturation period of 5 min at 94 °C, the following steps were repeated for 20 cycles in a thermal cycler (MyCycler thermocycler, Biorad): 1 min at 94 °C, 1 min at 60−72 °C, 10 min at 72 °C, followed by a final 10 min period at 72 °C. The amplified product was purified using GFX PCR DNA and Gel Band Purification kit (GE Healthcare). The final PCR product was digested with *Dpn*I to eliminate wild-type template and used to transform electrocompetent *E. coli* KRX cells. The presence of the desired mutation in the resulting plasmid and the absence of inadvertent additional mutations in other regions of the inset were confirmed by DNA sequencing.

"Activity-on-Plate" High-Throughput Screening. *E. coli* Tuner Δ*cueO*::*kan* cells harboring expression plasmids were grown overnight on solid TB medium supplemented with ampicillin (100 μg L$^{−1}$), kanamycin (10 μg L$^{−1}$), and 0.05 mM IPTG. Expression of the wild-type *mcoA* gene was initially tried using both the *E. coli* Tuner Δ*cueO*::*kan* and KRX Δ*cueO*::*kan* strains, but the use of the Tuner strain resulted in a 10 times higher number of transformants and was thus chosen for further

studies. Colonies were replica-plated onto chromatography paper (Whatman), and the original culture-plate was reincubated at 37 °C until colonies appeared (~5 h). The colonies on the filter papers were carefully lysed by soaking the chromatography paper in a solution with lysozyme (0.5 μg mL^{-1}) in 20 mM Tris-HCl buffer, pH 7.6. The filter papers were transferred to Petri dishes and incubated for 2 h at 37 °C. Then the filter papers were soaked in a solution containing 2.5 mM CuCl$_2$, to allow proteins to bind copper, and ABTS (2−10 mM) in 100 mM acetate buffer, pH 4, and incubated overnight at 43 °C. The variants showing increased enzymatic activities were identified by their dark green, gray, or purple color.

Expression of *mcoA* Variants in *E. coli* in 96-Well Plates. Colonies of the most active evolved variants screened using the "activity-on-plate" assay were picked from the original transformation plate and transferred to 96-well plates containing 200 μL of LB medium supplemented with ampicillin (100 μg L^{-1}) and kanamycin (10 μg L^{-1}). Only the central wells were used for cell growth while peripheral wells were filled with water in order to decrease evaporation. Four wells in each plate were used to inoculate the parental strain of each generation as controls. Cultures were incubated at 30 °C for 24 h, at 750 rpm in a Titramax 1000 shaker (Heidolph). Twenty microliters of the culture media was used to inoculate 96 well-plates containing fresh 180 μL TB medium supplemented with ampicillin (100 μg L^{-1}) and kanamycin (10 μg L^{-1}). Cultures were incubated at 750 rpm, at 30 °C for 3 h after which *mcoA* gene-expression was induced by adding 0.1 mM IPTG and 0.25 mM CuCl$_2$. Cultures were returned to the same cultivation conditions for another 4 h, after which the shaking was turned off.[37] Cultures were incubated overnight and cells were harvested by centrifugation (2750g for 20 min at 4 °C).

Cell Disruption in 96-Well Plates. McoA-producing cells were disrupted by resuspending cell pellets in 100 μL B-PER lysis solution (Bacterial Protein Extraction Reagent, Pierce). After centrifugation at 2750g for 30 min at 4 °C, the supernatants (cell crude extracts) were immediately used for activity measurements.

High-Throughput Screening in 96-Well Plates. Crude cells extracts (40 μL) were transferred into 96-well plates, and the activity was assayed by adding 160 μL of 100 mM acetate buffer, pH 4 containing 1 mM ABTS. The reaction was followed at 420 nm (ε = 36 000 M^{-1} cm^{-1}) on a Synergy 2 (Bioteck) microtiter plate reader. In the first two rounds of evolution, screening using end point mode after incubating the supernatants for 1 h in the presence of the substrate was required in order to detect activity. In the last two rounds, however, the initial activity was followed at 420 nm for only 5 min. Variants exhibiting the highest initial activity were rescreened to discard false positives. Mutations were verified by DNA sequencing analysis using T7 terminator universal primers. In each generation, the variant with the highest activity was chosen to be the parent for the next generation.

Production and Purification of WT and Variants. The genes coding for the WT and different variants, were cloned into pET21a (+) plasmid and introduced into the host strain *E. coli* Tuner Δ*cueO*::*kan* by electroporation. The recombinant strains were grown in LB medium supplemented with 100 μg mL^{-1} ampicillin and 10 μg mL^{-1} kanamycin, at 37 °C, 160 rpm. Gene-expression was induced, at OD$_{600\ nm}$ ~ 0.6, with 0.1 mM IPTG, and 0.25 mM CuCl$_2$ was added for full MCO-activity. After 4 h, agitation was stopped, and cells were incubated overnight at 25 °C. Cell cultures were collected by centrifugation (18 000g, 15 min at 4 °C). Cell pellets were suspended in 20 mM Tris-HCl

buffer, pH 7.6, containing 5 mM MgCl$_2$ and 1 U mL^{-1} of DNase I. Cells were disrupted by French Press (Thermo EFC), and lysates were centrifuged at 40 000g for 2 h at 4 °C. Cell crude extracts were incubated at 80 °C for 20 min, and denatured protein was removed by centrifugation (12 000g for 10 min). For 2B3, the resultant supernatant was loaded onto an ion exchange Q-Sepharose column equilibrated with 20 mM Tris-HCl, pH 7.6. Elution was carried out with a two-step linear NaCl gradient (0.0−0.5 and 0.5−1 M) in the same buffer. Fractions were collected and assayed for MCO-activity. Active fractions were pooled, concentrated, and applied on a Superdex 200 HR 10/30 column equilibrated with 20 mM Tris-HCl buffer, pH 7.6, containing 0.2 M NaCl. Active fractions were pooled, and enzyme concentration was estimated using the Abs$_{280\ nm}$ value.

UV−vis and CD Spectra. UV−visible absorption spectra of purified enzymes were obtained at room temperature in 20 mM Tris-HCl buffer, pH 7.6, using a Nicolet Evolution 300 spectrophotometer from Thermo Industries. CD spectra in the far-UV region were measured on a Jasco-720 spectrapolarimeter using a circular quartz cuvette with a 0.1 cm optical path length in the range of 190−260 nm. Protein content was 25 μM in 20 mM Tris-HCl buffer, pH 7.6.

Apparent Steady-State Kinetic Analysis. Maximal rates for oxidation of ABTS, syringaldazine (SGZ), 2,6-dimethoxyphenol (2,6-DMP), guaiacol, ferrous ammonium sulfate ($(NH_4)_2Fe(SO_4)_2 \cdot 6H_2O$), manganese chloride (MnCl$_2$), Mordant black 9 (MB9), Acid blue 62 (AB62), and Acid black 194 (AB194) (Table S2) were monitored at 40 °C using either a Nicolet Evolution 300 spectrophotometer or a Synergy2 microplate reader (BioTek). Oxidation of the various substrates was performed using the following conditions: in 100 mM sodium acetate buffer, pH 4, for ABTS (3 mM); in 100 mM sodium phosphate, pH 7, for SGZ (0.1 mM), 2,6-DMP (1 mM) and guaiacol (1 mM); in 100 mM sodium phosphate, pH 6, for MB 9 (2 mM), AB62 (2 mM), AB194 (2 mM) and in 100 mM MES buffer, pH 5, for ferrous ammonium sulfate (0.1 mM). Reactions were followed at 420 nm (ε_{ABTS} = 36,000 M^{-1} cm^{-1}), 530 nm (ε_{SGZ} = 65,000 M^{-1} cm^{-1}), 468 nm ($\varepsilon_{2,6-DMP}$ = 49,600 M^{-1} cm^{-1}), 470 nm ($\varepsilon_{Guaiacol}$ = 49,600 M^{-1} cm^{-1}), 550 nm (ε_{MB9} = 15,641 M^{-1} cm^{-1}), 600 nm (ε_{AB62} = 10,920 M^{-1} cm^{-1}), 570 nm (ε_{AB194} = 11,927 M^{-1} cm^{-1}) and 315 nm ($\varepsilon_{Fe(III)}$ = 2,200 M^{-1} cm^{-1}). Cuprous oxidase activity was measured in terms of rate of oxygen consumption by using an oxygen electrode (Oxygraph; Hansatech) at 40 °C as previously described.[14] Stock solutions of [Cu(I)(MeCN)$_4$]PF$_6$ were freshly prepared in argon-purged acetonitrile, and reactions were initiated by adding the substrate to an air-saturated mixture containing enzyme, 100 mM acetate buffer, pH 3.5. Apparent steady-state kinetic parameters (K_m and k_{cat}) were measured at 40 °C for ABTS (0.02−3 mM, pH 4), SGZ (2−75 μM, pH 7), Cu(I) (0.02−0.5 mM, pH 3.5), and Fe(II) (5−100 μM, pH 5), and kinetic data was fitted directly using the Michaelis−Menten equation (Origin software).

The enzymatic decolourisation of 3 anthraquinonic (Reactive blue 5, Disperse blue 1 and AB62) and 12 azo dyes (MB9, Mordant black 17, Mordant black 3, Acid black 194, Direct blue 1, Sudan orange G, Reactive red 4, Reactive black 5, Reactive yellow 145, Acid black 210, Acid orange 7 and Direct red 80) was monitored by measuring the differences between the initial and final absorbance at the λ_{max} for each dye. Reactions were performed at 37 °C in 96-well plates in 100 mM sodium phosphate, pH 6, with 2 mM of dye and 0.1 mg mL^{-1} of enzyme. The dependence on pH was tested using Britton Robinson buffer

(100 mM phosphoric acid, 100 mM boric acid and 100 mM acetic acid mixed with NaOH to desired pH range (4−8)).

Enzyme Stability Assays. Kinetic stability studies were performed as described previously.[7] In brief, enzyme solutions were incubated at 80 °C in 20 mM Tris-HCl buffer, pH 7.6, and at fixed time intervals, sample aliquots were withdrawn and tested for activity at 40 °C. Protein aggregation was monitored by measuring static light scattering with a Carry Eclipse spectrofluorimeter at 500 nm as excitation and emission wavelengths. Differential scanning calorimetry (DSC) measurements were carried out by VP-DSC from MicroCal at a scan rate of 1 °C/min. The experimental calorimetric races were obtained with 0.2 mg mL^{-1} of protein in 20 mM Tris-HCl buffer, pH 7.6 and 200 mM glycine buffer pH 3. The data were processed and fitted using Origin software supplied by the DSC manufacturer. The progress baseline-subtracted and concentration-normalized DSC curve was fitted to nontwo-state model with three transitions.

Other Methods. The copper content was determined through the trichloroacetic acid/bicinchoninic acid method of Brenner and Harris.[38] Protein identification was performed by MALDI-TOF/TOF, and the data was provided by the UniMS — Mass Spectrometry Unit, ITQB/IBET, Oeiras, Portugal. The molecular mass of the purified recombinant 2B3 protein was determined on a gel filtration Superose 12HR10/30 column (Amersham Biosciences) equilibrated with 20 mM Tris-HCl, pH 7.6, containing 0.2 M NaCl. Ribonuclease (13.7 kDa), chymotrypsinogen A (25 kDa), ovalbumin (43 kDa), albumin (67 kDa), and aldolase (158 kDa) were used as standards.

RESULTS AND DISCUSSION

Validation of High-Throughput Screenings and Optimization of Error-Prone PCR. An "activity-on-plate" high-throughput screening (HTS) was developed using *E. coli* overproducing wild-type McoA (Figure 1A). This approach, in
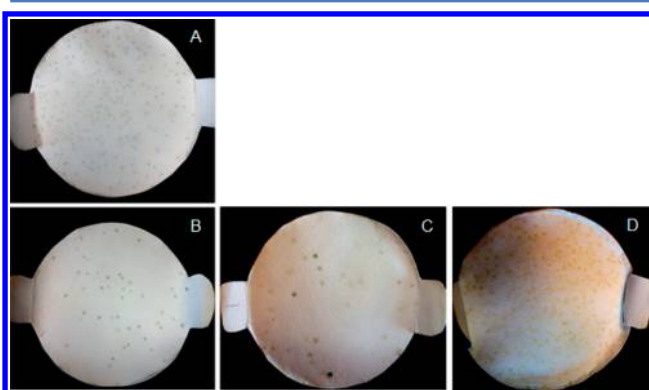

Figure 1. "Activity-on-plate" high-throughput assay (with 10 mM ABTS) using *E. coli* cells expressing wild-type *mcoA* (A) and mutant libraries constructed using ep-PCR in the presence of 0.1 mM MnCl$_2$ (B), 0.15 mM MnCl$_2$ (C), and 0.2−0.25 mM MnCl$_2$ (D).

spite of its qualitative nature, allows for the screening of a higher number of clones in a shorter period of time as compared to a standardized 96-well plate assay. Colonies showing a dark green or purple color (i.e., higher enzyme activity than wild-type) were rescreened using a quantitative activity-screening in 96-well plates. The differences in color are most likely due to the existence of two relatively stable and electrochemically reversible oxidation states of ABTS, namely, the cation radical, ABTS·$^+$

(green), and the dication, ABTS^{2+} (dark purple).[39] Coefficients of variance (CV = standard deviation/mean × 100%) of ≈13% were achieved for the final OD$_{600}$ of cell cultures in 96-well plates as well as for total protein content of crude extracts. A CV for maximal activity of ≈20% was reached, in six different 96-well plates, ensuring the required reproducibility of the *mcoA* expression system to pursue the directed evolution studies in spite of the low activity detected (5 × 10^{-3} U mg^{-1}) in crude extracts. Four libraries of *mcoA* mutant genes were constructed using different MnCl$_2$ concentrations in the error-prone PCR (ep-PCR) protocol with Taq polymerase and screened using ABTS (Figure 1B−D). The concentration of 0.15 mM MnCl$_2$ was chosen for the creation of further libraries because it resulted in a significant variation in activity (Figure 1C) and the desired mutation rate of 1−4 amino acid substitutions per gene.

Directed Evolution of McoA for Increased Catalytic Efficiency toward Aromatic Compounds. Four rounds of directed evolution were performed, and a total of approximately 94 000 clones were screened for activity using ABTS as a substrate (Figure 2). Random mutagenesis through ep-PCR was used to generate library diversity, and libraries of ∼20 000−30 000 variants were first screened using the "activity-on-plate" HTS. Variants identified showing enhanced activity were rescreened in 96-well plates (∼100−700 variants) using end point (for those from the first to the third generation) or kinetic (using the fourth generation variants) enzymatic assays. The parental variants for the following generations were selected on the basis of increased activity in crude extracts (Figure 2). Variant 2B3 was selected in the fourth generation, and the combined mutations gave a 37-fold improvement in activity in crude extracts compared with native enzyme. A fifth round of directed evolution was conducted with libraries constructed by using either ep-PCR using the 2B3 variant gene or DNA shuffling (using three variants from the fourth generation, Figure 2). Unfortunately, even after several attempts, no variants with significantly improved enzymatic activity were identified. Therefore, the variant 2B3 obtained in the fourth generation was produced in *E. coli* (Δ*cueO*) in a batch scale, purified from the soluble fraction using a heat treatment step and kinetically and biochemically characterized.

Interestingly, the evolved 2B3 variant was produced in a soluble form, and purification from crude extracts resulted in >3-fold higher enzyme yield (2 mg L^{-1}; Figure S1) when compared to the recombinant wild-type McoA. This latter was mostly produced in *E. coli* in the form of inclusion bodies, which required purification using laborious *in vitro* refolding approaches and resulted in a final yield of 0.6 mg L^{-1}.[14] Purified 2B3 protein migrated in SDS-PAGE as two major bands of ∼35 and 59 kDa (Figure S1A); however, a single peak was eluted from exclusion size chromatography with the molecular mass of ∼57 kDa, close to the theoretical value predicted from the *mcoA* gene sequence (59.5 kDa) (Figure S1B). Moreover, the two bands were identified as McoA using MALDI-TOF/TOF analysis with sequence coverage of 37% after tryptic digestion. Therefore, we infer that the ∼59 kDa form in the SDS-PAGE represents the fully denatured form and the faster migrating ∼35 kDa species most likely represents a partially unfolded form of the enzyme. In fact, only the 35 kDa form was seen in the SDS-PAGE denaturing buffer if the purified protein was left at room temperature, although the treatment of the protein preparation for 10 to 60 min at 100 °C caused the appearance of the ∼59 kDa band (data not shown). Incomplete denaturation by SDS treatment has also been reported for some extremely thermostable enzymes
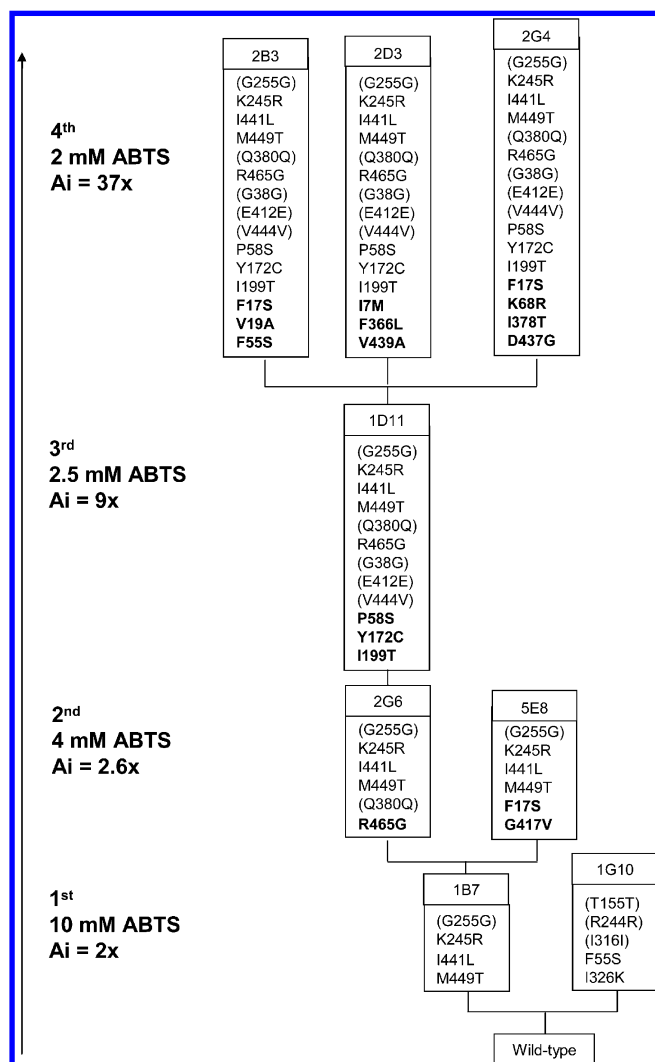
Figure 2. Lineage of McoA variants generated in this study. In the 1st generation, a total of 29 831 clones were screened using 10 mM ABTS in the "activity-on-plate" HTS, and 657 variants were identified showing enhanced activity. These mutant strains were rescreened in 96-well plates, and the 1B7 variant was selected on the basis of its 2-fold increased activity in crude extracts when compared to the parental wild-type extracts. Next, the 2nd generation was evolved from the 1B7 variant as "parent". The ABTS concentration was adjusted to 4 mM, and 23 891 clones were screened from which 259 variants were rescreened in 96-well plates. The 2G6 variant was identified having a slightly higher activity (1.3-fold) when compared to its parental strain (1B7). In the 3rd generation, 22 204 clones were screened in the "activity-on-plate" HTS using 2.5 mM of ABTS; 162 variants were rescreened for activity. This led to selection of variant 1D11 showing a 4-fold higher activity for ABTS as compared to its parent (2G6). In the 4th generation, the ABTS concentration was diminished to 2 mM, and the screening of 18 052 clones resulted in the selection of 108 variants. From these, variant 2B3 was selected on the basis of a 4-fold higher activity than the parental strain (1D11). New nonsynonymous mutations are indicated in bold and synonymous mutations are between brackets.

purified from hyperthermophilic microorganisms,[7,40] suggesting that 2B3 variant may be more thermostable than the wild-type McoA. The purified 2B3 contained a full complement of copper, with a ratio of ~4 mol of copper per mol of protein, and exhibited an absorption maximum at 600 nm that corresponds to the Cu–Cys interaction at the T1 Cu center (Figure S2A). Circular dichroism (CD) spectra in the far-UV region of the 2B3 variant

was similar to the wild-type enzyme, rich in β-sheets with a negative peak at 216–224 (Figure S2B), reflecting the typical secondary structure found in MCOs. A secondary structure with 12% α-helical, 28% β-strand, and more than 60% of turns and random coil structure was estimated via the CDSSTR method.[41]

2B3McoA Variant Possesses Laccase-Activity. The apparent steady-state kinetic parameters of the purified 2B3 variant were measured for two aromatic substrates, ABTS and SGZ, and for the metal ions, Cu(I) and Fe(II) (Table 1). The

Table 1. Apparent Steady-State Kinetic Parameters of Wild-Type McoA and Its Evolved 2B3 Variant for the Oxidation of Metal Ions and Organic Substrates at 40°C in the Absence of Exogenous Cu(II) in the Reaction Mixture

|	substrates	k_{cat} (s^{-1})	K_m (mM)	k_{cat}/K_m (s^{-1} M^{-1})
wild-type	Cu(I)[a]	2.3 ± 0.5	0.10 ± 0.02	2.3 × 10^4
	Fe(II)[b]	0.2 ± 0.1	0.008 ± 0.001	2.5 × 10^4
	ABTS[c]	2.2 ± 0.1	1 ± 0.1	3.3 × 10^3
	SGZ[d]	ND[e]	-	-
2B3	Cu(I)[a]	5 ± 1	0.3 ± 0.1	2.0 × 10^4
	Fe(II)[b]	ND	-	-
	ABTS[c]	211 ± 10	0.9 ± 0.1	2.4 × 10^5
	SGZ[d]	0.040 ± 0.001	0.008 ± 0.001	5.0 × 10^3

ND — not detected. [a]100 mM sodium acetate, pH 3.5. [b]100 mM MES buffer, pH 5. [c]100 mM sodium acetate, pH 4. [d]100 mM sodium phosphate, pH 7. [e]No activity was detected for SGZ in the absence of exogeneous Cu(II); in the presence of 0.1 mM Cu(II), a residual activity of 0.0010 ± 0.0002 U mg^{-1} was measured.

obtained values indicated that the laboratory evolution of McoA changed its enzymatic activity from a metallo-oxidase to a laccase; its specificity constant or catalytic efficiency for ABTS (k_{cat}/K_m) increased about 100-fold when compared to the wild-type enzyme and is 10-fold higher than that for Cu(I) oxidation. Moreover, the activity for Fe(II) oxidation was strongly diminished, and oxidation of the phenolic SGZ by this variant was significant, in contrast to the wild-type enzyme, which is inactive for this substrate in the absence of exogenous copper in the reaction mixture. Interestingly the catalytic efficiency for Cu(I) remains similar to the wild-type protein. The achieved catalytic efficiency for ABTS oxidation (2.4 × 10^5 s^{-1} M^{-1}) was approximating that observed for the wild-type CotA-laccase[42] (1.2 × 10^6 s^{-1} M^{-1}) and of evolved laccases from *B. subtilis*[43] (7 × 10^7 s^{-1} M^{-1}), *Myceliophthora thermophile*[44] (1 × 10^2 s^{-1} M^{-1}), and *Pleutotus ostreatus*[45] (6 × 10^6 s^{-1} M^{-1}). In all cases, the reported improvement of the efficiencies (k_{cat}/K_m) were due to an increase in the k_{cat} parameter. Maximal enzymatic activity in the 2B3 variant was independent of the presence of copper in the reaction assay, in contrast to what was previously reported for the wild-type McoA enzyme.[14] The catalytic efficiency of the 2B3 variant was further investigated using a range of possible aromatic substrates including the phenolic compounds 2,6-DMP, guaiacol and a few anthraquinonic and azo dyes (Table 2 and Table S2). The 2B3 variant exhibited activity not only for both phenolics, but it also showed significant oxidation rates for synthetic dyes, similar to those achieved by CotA-laccase.[46] Moreover, it oxidatively bleached 15 synthetic dyes at different extents in contrast to wild-type McoA enzyme, which exhibited decolorizing activity for only 7 synthetic dyes (Figure 3A). Noteworthy, the catalytic activity of the 2B3 variant using dyes as substrates is measurable over a wide range of pH values (from pH 4 to pH 8) (Figure 3B) in contrast to what has been reported for other

Table 2. Maximal Rates of Purified Wild-Type McoA and Its Evolved 2B3 Variant for Metal Ions and Various Aromatic Substrates

substrate	V_{max} (U mg^{-1})	
	wild-type	2B3
Cu(I)	2.3 ± 0.2	5 ± 1
Fe(II)	0.3 ± 0.1	ND
ABTS	2.2 ± 0.1	211 ± 10
SGZ	ND	0.040 ± 0.001
DMP	ND	0.10 ± 0.01
Guaiacol	ND	0.040 ± 0.004
Mordant Black 9	0.41 ± 0.04	1.0 ± 0.1
Acid Blue 62	0.027 ± 0.003	0.37 ± 0.04
Acid black 194	0.017 ± 0.003	0.07 ± 0.01

ND − not detected.
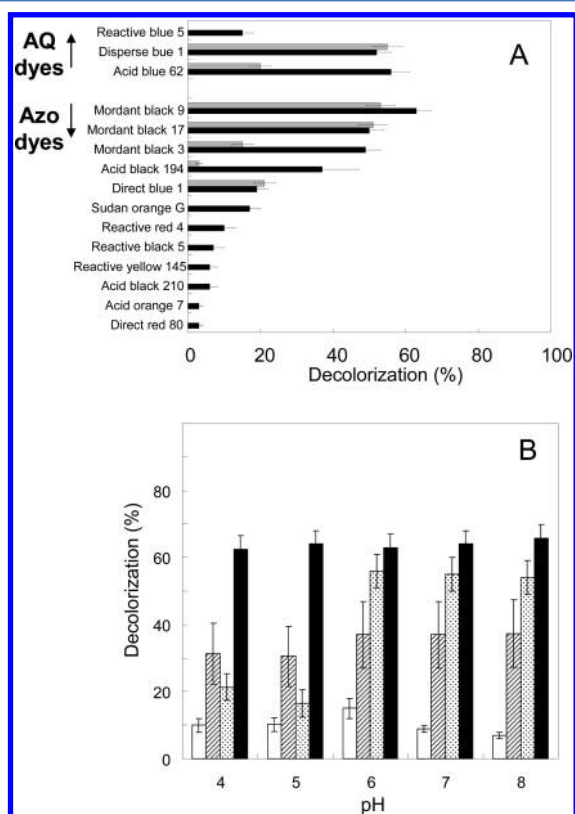
Figure 3. (A) Decolorization of anthraquinone (AQ) and azo dyes after 24 h of reaction using wild-type McoA (grey bars) and the 2B3 variant (white bars) in 100 mM sodium phosphate, pH 6. (B) Decolorization of Reactive blue 5 (black bars), Acid black 194 (dashed bars), Acid blue 62 (light gray), and Mordant black 9 (black bars) by the 2B3 variant in a pH range of 4 to 8 in Britton Robinson buffer. Reactions were performed at 37 °C with 2 mM of dye and 0.1 mg mL^{-1} of enzyme.

laccases; CotA-laccase shows an optimum at pH 8−9 and no detectable decolorization below pH 5,[47] whereas the majority of fungal laccases show optimal for dye degradation in the acidic pH range (from pH 4 to 6).[48−50]

2B3McoA Variant Is a Thermoactive and Hyper-thermostable Laccase. The 2B3 variant reached an activity optimum at temperatures around 70−75 °C (Figure S3), similar to the one observed for the wild-type.[14] It is remarkable that, even though the enzyme was repeatedly evolved for higher activity for ABTS, the specificity of the variants changed without

loss of thermophily (i.e., showing only minor stability−activity trade-offs). This is most likely related to alterations in conformational flexibility to mediate new functions that occur without severely compromising the conformation governing the previously existing functions.[51] Interestingly, the 2B3 variant was dramatically less aggregation-prone than wild-type McoA: the variant deactivates at 80 °C according to a first-order kinetics (Figure 4A and inset) unlike the wild-type enzyme where the activity decay at 80 °C occurs in two steps: (i) a first deactivation step that last for 1 h assigned to an aggregation process, resulting in an intermediate state with 50% of the initial activity, and (ii) the slowly deactivation of this intermediate (with a lifetime of 8 h) to the final denatured state.[14] Static light scattering confirmed that the 2B3 variant did not aggregate up to 120 °C, the highest temperature tested (Figure 4B). Moreover, 50% of activity was retained after 5 h at 80 °C, 5- and 2-fold improvements when compared to the wild-type McoA and CotA-laccase, respectively.[37] Therefore, the thermal deactivation of the 2B3 variant can be described by the classical Lumry−Eyring model (N ↔ U → D, where N, U, and D stand for the folded, the unfolded, and the denatured enzyme, respectively) in contrast to the kinetic partitioning between aggregation and unfolding observed for the wild-type.[12] A similar large improve in the kinetic stability associated with increased resistance to aggregation of a FMN-dependent NADPH:dye/quinone oxidoredutase (azoreductase) variant created by directed evolution was recently reported.[52]

The thermodynamic stability probed by differential scanning calorimetry (DSC) showed that the 2B3 variant did not unfold up to 120 °C at pH 3. Wild-type McoA exhibits an endothermic peak at pH 3 that was fitted using a non-two-state model with three independent transitions, with melting temperatures (temperature at which 50% of the molecules are unfolded) at 105, 110, and 114 °C.[12] Precipitation before unfolding was observed at pH values higher than 3 in McoA wild-type;[12] however, we have not detected this behavior in the present study, and the thermal stability of the tertiary structure of both wild type and 2B3 were probed by DSC at pH 7.6. The DSC thermogram of wild type showed the typical protein aggregation fingerprint characterized by a drop in the baseline after the endothermic peak leading to 100% of irreversibility and T_m of ∼77, 81, 84 °C could be roughly estimated (Figure 4C). The variant 2B3 did not aggregate after thermal unfolding and displayed three distinct endothermic transitions showing slightly higher T_m values of 82, 84, 86 °C (Figure 4C).

Molecular Details of Mutations That Change McoA Substrate Specificity or Improve Enzyme Solubility. The vast majority of nonsynonymous amino acid changes identified in the 2B3 variant are spread on or near the protein surface (nine out of ten), and eight of them occurred in loops (Figure 5), based on the McoA model structure.[14] Four of the substitutions, located on surface loops, resulted in serine residues or in other residues bearing a hydroxyl group (F17S, F55S, P58S, and I199T), possibly increasing surface hydrophilicity. Two of these changes, F55S and P58S, are located in one loop, Ser41 to Gly60, are not modeled because no counterparts were found in the template structures.[14] The analysis of the five synonymous mutations accumulated show that the codon exchanged in mutations G38G and G255G (GGT → GGC) resulted in similar frequencies of codon usage as compared with the wild-type. In contrast, the mutation E412E (GAA → GAG) leads to a codon that has a lower percentage of usage (31.7%) as compared with the wild-type codon (68.3%) and the two mutations Q380Q and
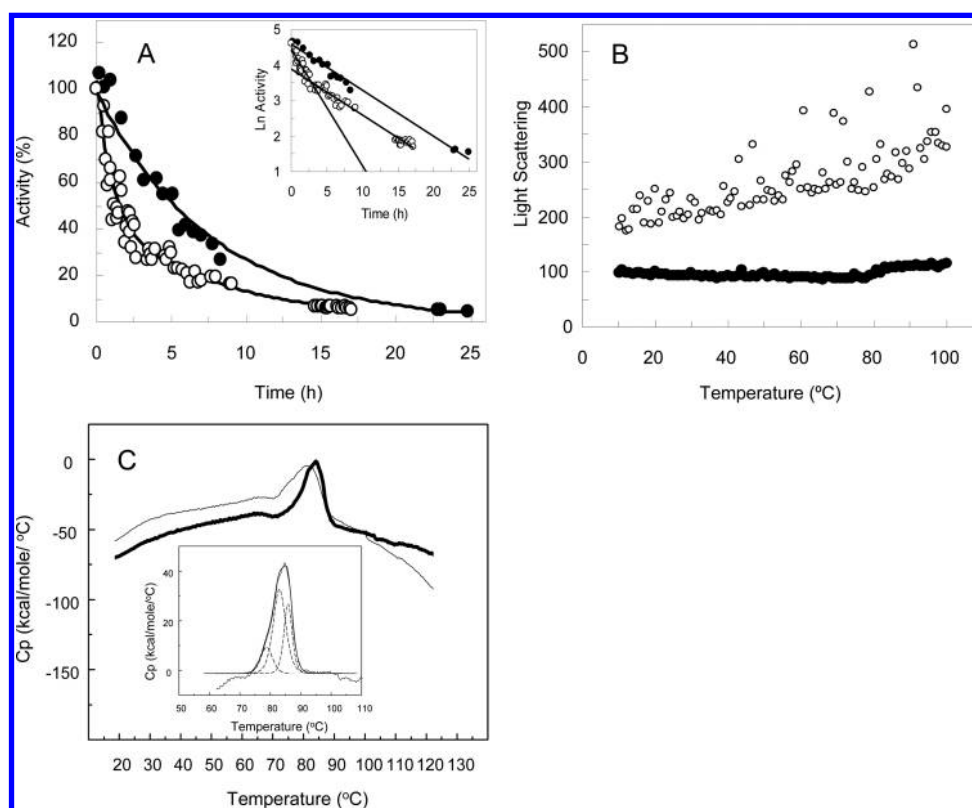
Figure 4. (A) Kinetic stability of wild-type (open circles) and the 2B3 variant (closed circles) at 80 °C. (B) Static light scattering of wild-type (open circles) and the 2B3 variant (closed circles). (C) Excess heat capacity of McoA and the 2B3 variant obtained from differential scanning calorimetry at pH 7.6. The thick line (experimental data of 2B3) was fitted with three independent transitions shown separately in thin lines.
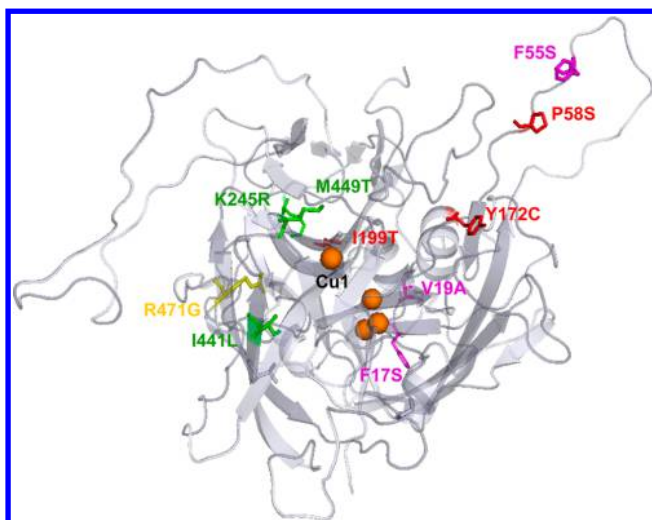
Figure 5. Mapping of the amino acids identified in the 2B3 variant using the model structure of the *A. aeolicus* McoA derived by comparative modeling techniques.[14] Mutations acquired in the 1st generation are indicated in green, those from the 2nd generation in orange, from the 3rd in red, and from the 4th generation in purple.

V444 V favored codon usage CAA (33.5%) → CAT (66.5%) and GTA (15.9%) → GTG (36.2%), respectively, which could potentially enhance the heterologous variants expression.

In order to investigate which nonsynonymous mutations would contribute to the improved properties of the 2B3 variant, nine single variants containing mutations accumulated in the evolution process were constructed from wild-type by site-directed mutagenesis (except for F17S due to technical

constraints). These variants were overproduced in *E. coli* and partially purified after incubation of crude extracts at 80 °C for 20 min. The kinetic characterization of variants showed that all mutations, except P58S that resulted in a 3-fold lower activity, led to increased activity for ABTS as compared to wild-type (Table 3); notably, two mutations I441L and I119T, introduced in the first and third generation, respectively, yielded in 6 to 17 higher activity to the wild-type. Interestingly, all variants showed increased half-lives at 90 °C as compared to wild-type (Table 3). Moreover, except for M449T, where a two-step decay in activity was observed upon incubation at 90 °C, the remaining variants deactivates according to a first-order kinetics and therefore

Table 3. Activity (V_{max}) and Kinetic Stability ($t_{1/2}$ at 90°C) of Partially Purified Preparations of Wild-Type McoA and Single Variants

	activity	stability	
proteins	ABTS (U mg^{-1})	lifetime of the 1st step/$t_{1/2}$ intermediate* at 90 °C (h)	$t_{1/2}$ at 90 °C (h)
wild-type	0.038 ± 0.004	0.65 ± 0.1/14 ± 3	-
M449T	0.06 ± 0.01	0.25 ± 0.05/18 ± 2	-
I441L	0.2 ± 0.1	-	6 ± 1
K245R	0.11 ± 0.01	-	5.1 ± 0.1
R471G	0.07 ± 0.01	-	6 ± 1
P58S	0.011 ± 0.001	-	13 ± 1
I199T	0.6 ± 0.1	-	7 ± 1
Y172C	0.09 ± 0.01	-	9 ± 1
V19A	0.05 ± 0.01	-	15 ± 3
F55S	0.05 ± 0.01	-	9.9 ± 0.1

*The intermediate shows ~50% of the initial activity.

Table 4. Activity (V_{max}), Kinetic ($t_{1/2}$ at 90°C), and Thermodynamic Stability (T_m) of Partially Purified Preparations of Wild-Type McoA and Its Variants

proteins	activity			stability		
	Cu (I) (U mg^{-1})	Fe (II) (mU mg^{-1})	ABTS (U mg^{-1})	lifetime of the 1st step/$t_{1/2}$ intermediate* at 90 °C (h)	$t_{1/2}$ at 90 °C (h)	T_m at pH 7.6 (°C)
Wild-type	0.10 ± 0.01	3.2 ± 0.3	0.038 ± 0.004	0.7 ± 0.1/14 ± 3	-	~77, 81, 84
1B7	0.08 ± 0.01	3 ± 1	0.37 ± 0.04	0.5 ± 0.1/14 ± 1	-	~78, 82, 85
2G6	0.08 ± 0.01	6.6 ± 0.3	0.29 ± 0.03	0.5 ± 0.1/11.3 ± 0.4	-	~80, 83, 86
2G6-P58S	nd	3.9 ± 0.3	0.32 ± 0.03	0.5 ± 0.1/7.0 ± 0.1	-	nd
2G6-Y172C	nd	2.3 ± 0.4	0.17 ± 0.02	-	6 ± 1	nd
2G6-I199T	nd	2 ± 1	1.7 ± 0.1	-	6 ± 1	nd
2G6-I199T/ Y172C	nd	3.8 ± 0.4	2.8 ± 0.2	-	4.9 ± 0.1	nd
2G6-I199T/P58S	nd	5 ± 1	1.11 ± 0.04	-	5 ± 1	nd
1D11	0.10 ± 0.01	2.9 ± 0.3	1.35 ± 0.13	-	7 ± 1	~80, 84, 86
1D11-F17S	nd	2 ± 1	4.7 ± 0.1	-	5.4 ± 0.4	~80, 84, 86
1D11-V19A	nd	1.5 ± 0.3	4.7 ± 0.2	-	5.1 ± 0.1	80, 84, 86
1D11-F55S	nd	4 ± 1	4.7 ± 0.2	-	5.2 ± 0.2	~80, 84, 86
2B3	0.09 ± 0.01	0.4 ± 0.1	21 ± 2	-	5.7 ± 0.3	82, 84, 86

nd − not determined. *The intermediate shows ~50% of the initial activity.

seemed to be able to individually contribute to the abolishment of protein aggregation in the wild-type McoA (Figure 4A).

In the next step, we have assessed the synergistic effect of single mutations, and for that we have constructed and characterized single and double variants of the hits of the second (2G6) and third generation (1D11) (Table 4); please note that the hit of the second generation (2G6) showed only one additional mutation in relation to the hit of the first generation (1B7). 1B7 from the first generation yielded a 10-fold improved activity for ABTS in comparison to the wild-type, most likely related with the observed positive effects of single M449T, K245R, and I449L substitutions in the activity for ABTS (Table 3). The replacement of R471 by a Gly in the second generation, as assessed by examining the 2G6 variant, seemed to mostly impact the thermodynamic stability of the enzyme, leading to higher melting temperatures, because a slightly lower activity and similar kinetic stability was observed in this variant as in 1B7 variant.

The results of the insertion of single and double substitutions in 2G6 confirmed the "leading" role of I199T toward an altered specificity in the evolution process of McoA, because its presence firmly correlated with increased activity for ABTS (4 to 10 times). Substitution of Y172C appeared to synergistically interact with I199T, because the 2G6 double Y172C−I199T variant almost doubled its activity in comparison to the 2G6 single I199T variant. The role of P58S in the 2G6 background seemed neutral or even antagonistic, considering the similar or (2-fold) lower activity observed in 2G6 and 2G6-I199T variants, respectively. This is in agreement with results presented in Table 3, where replacement of P58S in wild-type resulted in the lowest measured ABTS activity; even though the half-life at 90 °C (13 h) corresponded to a 2-fold increased stability as compared to mutations introduced in the early stages of the evolution. As previously mentioned, all mutations but M499T are thought to individually contribute to the increased "solubilization" of the enzyme, as suggested by the single-step temperature deactivation profiles exhibited (Table 3); however, in the evolution process, this behavior was only observed upon substitution (and following synergism) of Y172C and I199T residues in the third generation (Table 4).

The single replacements of F17S, V19A, and F55S in the 1D11 variant resulted in 3-fold improvements in the activity for ABTS, and thus, we can propose the occurrence of a further synergistic interaction among these residues explaining the 20-fold increased activity measured in 2B3 in comparison to the 1D11 variant (Table 4). Conversely, 2B3 showed a 10-fold lower activity for Fe(II) as compared to those exhibited by 1D11 single F17S, V19A, and F55S variants (Table 4). Maintaining similar levels of activity for Cu(I) in the 2B3variant and in the wild-type as well as the residual activity for ferrous iron oxidation (Table 4) suggest that in McoA these transition metals do not share the same substrate binding sites. The methionine-rich regions present in many bacterial MCOs,[6] reminiscent of those found in copper homeostasis proteins,[54,55] are considered "cuprous oxidase" motifs, although carboxylate residues close to the T1 Cu center as in the yeast Fet3p are viewed as "ferroxidase motifs".[2,3] In the model structure of McoA, a methionine-rich segment (Phe 321-Val 363) was observed close to the T1 Cu site,[14] and the maintenance of the Cu(I) activity in the outperforming 2B3 variant most likely related with the absence of substitutions in this Met-rich segment; however, the structural reasons for abrogating Fe(II) oxidation are not obvious at this point. In this context, the apparent critical role of V19A substitution as determinant of stability is worth mentioning for explaining the differences observed in the 2B3 variant unfolding mechanism. The differential thermogram of 1D11 with an additional V19A single mutation did not exhibit, similarly to 2B3 and unlike the other examined variants, the typical protein aggregation fingerprint (i.e., the drop in the baseline after the endothermic peak; Figure 6). This finding correlated well with the highest stability measured in the single V19A variant ($t_{1/2}$ = 15 h at 90 °C, Table 3).

Overall, our results show that although the directed evolution strategy was based on occurrence of a considerable number of mutation events (i.e., after 4 cycles the final variant accumulated 15 mutations (5 silent)), all mutations introduced appear essential for the hit 2B3 variant properties, except eventually for the synonymous E412E and nonsynonymous P58S substitutions. Therefore, McoA seems to have essentially been evolved through sequential introduction of beneficial mutations.[51,55] Mutations M449T, K245R, I441L, Y172C, V19A, F55S, and in
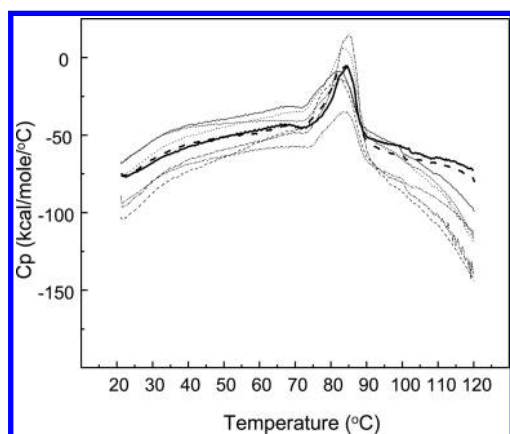
Figure 6. Excess heat capacity of McoA (solid thin line) and its variants 1B7 (dashed thin line), 2G6 (dot line), 1D11 (dashed thin dot), 1D11-F17S (dashed dot dot thin line), 1D11-V19A (dashed thick line), 1D11-F55S (short dashed thin line), and 2B3 (solid thick line) obtained from differential scanning calorimetry at pH 7.6.

particular I199T have likely contributed individually or synergistically to the improvement of the oxidation rates for aromatic substrates. Similarly, the substitution of R471G and especially V19A, to smaller amino acid residues, with a potential benefit of releasing of conformational strain, appears particularly significant in the stabilization of the enzyme during the *in vitro* evolution.

CONCLUDING REMARKS

Laccases are the most promising enzymes for lignin degradation and successful valorization due to (i) the low cost of introducing O_2 as primary oxidant, and (ii) the possibility of controlling reactivity by increasing or quenching O_2 partial pressure in process conditions. Bacterial laccases, although less known and utilized biocatalysts compared to their fungal counterparts, are able to perform analogous reactions while benefiting from higher optimal temperature and pH-range, salt tolerance, and increased stability. Additionally, bacterial systems have well-established genetic and molecular biological tools allowing for higher enzyme production yields and application of protein engineering tools. The evolved 2B3 variant reported here shows considerable catalytic efficiency for ABTS comparable to other well-known laccases and coupled with its enhanced stability, solubility, and easiness of purification is potentially useful for biotechnological applications. It is notable that this variant is potentially an excellent candidate to be further evolved for new specificities and applications considering that the additional stability confers the ability to accommodate the often destabilizing mutations that are required for the acquisition of new and improved functions.[57] Such studies will also allow for a better insight into the structure–function relationships within the multicopper oxidase family of enzymes including the features and mechanisms behind their multifunctionality. This has several general implications in the understanding of molecular recognition of ligands, for example, for drug discovery programs and for the engineering of proteins in the realm of biotechnology, including the field of synthetic biology.

ASSOCIATED CONTENT

Ⓢ Supporting Information

The Supporting Information is available free of charge on the ACS Publications website at DOI: 10.1021/acscatal.5b00771.

Supplemental tables and additional figures (Tables S1 and S2; Figures S1−S3) (PDF)

AUTHOR INFORMATION

Corresponding Author

*E-mail: lmartins@itqb.unl.pt.

Notes

The authors declare no competing financial interest.

ACKNOWLEDGMENTS

REFERENCES

(1) Jones, S. M.; Solomon, E. I. *Cell. Mol. Life Sci.* **2015**, *72*, 869−883.

(2) Kosman, D. J. *JBIC, J. Biol. Inorg. Chem.* **2010**, *15*, 15−28.

(3) Stoj, C. S.; Kosman, D. J. In *Encyclopedia of Inorganic Chemistry*, 2nd ed.; King, R. B., Ed.; John Wiley & Sons: Hoboken, NJ, 2005; Vol. *II*, pp 1134−1159.

(4) Kunamneni, A.; Plou, F. J.; Ballesteros, A.; Alcalde, M. *Recent Pat. Biotechnol.* **2008**, *2*, 10−24.

(5) Pezzella, C.; Guarino, L.; Piscitelli, A. *Cell. Mol. Life Sci.* **2015**, *72*, 923−940.

(6) Martins, L. O.; Durao, P.; Brissos, V.; Lindley, P. F. *Cell. Mol. Life Sci.* **2015**, *72*, 911−922.

(7) Martins, L. O.; Soares, C. M.; Pereira, M. M.; Teixeira, M.; Costa, T.; Jones, G. H.; Henriques, A. O. *J. Biol. Chem.* **2002**, *277*, 18849−18859.

(8) Sousa, A. C.; Martins, L. O.; Robalo, M. P. *Adv. Synth. Catal.* **2013**, *355*, 2908−2917.

(9) Sousa, A. C.; Oliveira, M. C.; Martins, L. O.; Robalo, M. P. *Green Chem.* **2014**, *16*, 4127−4136.

(10) Sousa, A. C.; Piedade, M. F. M. M.; Martins, L. O.; Robalo, M. P. *Green Chem.* **2015**, *17*, 1429−1433.

(11) Silva, C. S.; Durao, P.; Fillat, A.; Lindley, P. F.; Martins, L. O.; Bento, I. *Metallomics* **2012**, *4*, 37−47.

(12) Fernandes, A. T.; Martins, L. O.; Melo, E. P. *Biochim. Biophys. Acta, Proteins Proteomics* **2009**, *1794*, 75−83.

(13) Fernandes, A. T.; Damas, J. M.; Todorovic, S.; Huber, R.; Baratto, M. C.; Pogni, R.; Soares, C. M.; Martins, L. O. *FEBS J.* **2010**, *277*, 3176−3189.

(14) Fernandes, A. T.; Soares, C. M.; Pereira, M. M.; Huber, R.; Grass, G.; Martins, L. O. *FEBS J.* **2007**, *274*, 2683−2694.

(15) Singh, S. K.; Grass, G.; Rensing, C.; Montfort, W. R. *J. Bacteriol.* **2004**, *186*, 7815−7817.

(16) Stoj, C.; Kosman, D. J. *FEBS Lett.* **2003**, *554*, 422−426.

(17) Hildén, K.; Hakala, T. K.; Lundell, T. *Biotechnol. Lett.* **2009**, *31*, 1117−1128.

(18) Currin, A.; Swainston, N.; Day, P. J.; Kell, D. B. *Chem. Soc. Rev.* **2015**, *44*, 1172−1239.

(19) Dalby, P. A. *Curr. Opin. Struct. Biol.* **2011**, *21*, 473−480.

(20) Romero, P. A.; Arnold, F. H. *Nat. Rev. Mol. Cell Biol.* **2009**, *10*, 866−876.

(21) Cho, C. M. H.; Mulchandani, A.; Chen, W. *Appl. Environ. Microb* **2004**, *70*, 4681−4685.

(22) Aharoni, A.; Gaidukov, L.; Khersonsky, O.; Gould, S. Mc. Q.; Roodveldt, C.; Tawfik, D. S. *Nat. Genet.* **2005**, *37*, 73−76.

(23) Liu, C.; Yang, G. Y.; Wu, L.; Tian, G. H.; Zhang, Z. M.; Feng, Y. *Protein Cell* **2011**, *2*, 497−506.

(24) Williams, G. J.; Zhang, C.; Thorson, J. S. *Nat. Chem. Biol.* **2007**, *3*, 657−662.

(25) Molloy, S.; Nikodinovic-Runic, J.; Martin, L. B.; Hartmann, H.; Solano, F.; Decker, H.; O'Connor, K. E. *Biotechnol. Bioeng.* **2013**, *110*, 1849−1857.

(26) Mate, D. M.; Alcalde, M. *Biotechnol. Adv.* **2015**, *33*, 25−40.

(27) Pardo, I.; Camarero, S. *Cell. Mol. Life Sci.* **2015**, *72*, 897−910.

(28) Gupta, N.; Lee, F. S.; Farinas, E. T. *J. Mol. Catal. B: Enzym.* **2010**, *62*, 230−234.

(29) Koschorreck, K.; Schmid, R. D.; Urlacher, V. B. *BMC Biotechnol.* **2009**, *9*, 12.

(30) Toscano, M. D.; De Maria, L.; Lobedanz, S.; Ostergaard, L. H. *ChemBioChem* **2013**, *14*, 1209−1211.

(31) Festa, G.; Autore, F.; Fraternali, F.; Giardina, P.; Sannia, G. *Proteins: Struct., Funct., Genet.* **2008**, *72*, 25−34.

(32) Jia, H.; Lee, F. S.; Farinas, E. T. *ACS Comb. Sci.* **2014**, *16*, 665−669.

(33) Grass, G.; Rensing, C. *Biochem. Biophys. Res. Commun.* **2001**, *286*, 902−908.

(34) Grass, G.; Rensing, C. *J. Bacteriol.* **2001**, *183*, 2145−2147.

(35) Joern, J. M. In *Directed evolution library creation: methods and protocols*; Arnold, F. H., Georgiou, G., Eds.; Humana Press: Totowa, New Jersey, 2003; Vol. *231*, pp 85−89.

(36) Zhao, H.; Arnold, F. H. *Nucleic Acids Res.* **1997**, *25*, 1307−1308.

(37) Durão, P.; Chen, Z.; Fernandes, A. T.; Hildebrandt, P.; Murgida, D. H.; Todorovic, S.; Pereira, M. M.; Melo, E. P.; Martins, L. O. *JBIC, J. Biol. Inorg. Chem.* **2008**, *13*, 183−193.

(38) Brenner, A. J.; Harris, E. D. *Anal. Biochem.* **1995**, *226*, 80−84.

(39) Bourbonnais, R.; Leech, D.; Paice, M. G. *Biochim. Biophys. Acta, Gen. Subj.* **1998**, *1379*, 381−390.

(40) Dong, G.; Vieille, C.; Zeikus, J. G. *Appl. Environ. Microbiol.* **1997**, *63*, 3577−3584.

(41) Sreerama, N.; Woody, R. W. *Anal. Biochem.* **2000**, *287*, 252−260.

(42) Brissos, V.; Chen, Z.; Martins, L. O. *Dalton Trans* **2012**, *41*, 6247−6255.

(43) Gupta, N.; Farinas, E. T. *Protein Eng., Des. Sel.* **2010**, *23*, 679−682.

(44) Bulter, T.; Alcalde, M.; Sieber, V.; Meinhold, P.; Schlachtbauer, C.; Arnold, F. H. *Appl. Environ. Microbiol.* **2003**, *69*, 987−995.

(45) Miele, A.; Giardina, P.; Sannia, G.; Faraco, V. *J. Appl. Microbiol.* **2010**, *108*, 998−1006.

(46) Santos, A.; Mendes, S.; Brissos, V.; Martins, L. O. *Appl. Microbiol. Biotechnol.* **2014**, *98*, 2053−2065.

(47) Pereira, L.; Coelho, A. V.; Viegas, C. A.; dos Santos, M. M. C.; Robalo, M. P.; Martins, L. O. *J. Biotechnol.* **2009**, *139*, 68−77.

(48) Camarero, S.; Ibarra, D.; Martinez, M. J.; Martinez, A. T. *Appl. Environ. Microbiol.* **2005**, *71*, 1775−1784.

(49) Kandelbauer, A.; Erlacher, A.; Cavaco-Paulo, A.; Guebitz, G. M. *Biocatal. Biotransform.* **2004**, *22*, 331−339.

(50) Pogni, R.; Brogioni, B.; Baratto, M. C.; Sinicropi, A.; Giardina, P.; Pezzella, C.; Sannia, G.; Basosi, R. *Biocatal. Biotransform.* **2007**, *25*, 269−275.

(51) Soskine, M.; Tawfik, D. S. *Nat. Rev. Genet.* **2010**, *11*, 572−582.

(52) Brissos, V.; Goncalves, N.; Melo, E. P.; Martins, L. O. *PLoS One* **2014**, *9*, e87209.

(53) Arnesano, F.; Banci, L.; Bertini, I.; Thompsett, A. R. *Structure* **2002**, *10*, 1337−1347.

(54) Huffman, D. L.; Huyett, J.; Outten, F. W.; Doan, P. E.; Finney, L. A.; Hoffman, B. M.; O'Halloran, T. V. *Biochemistry* **2002**, *41*, 10046−10055.

(55) Bloom, J. D.; Arnold, F. H. *Proc. Natl. Acad. Sci. U. S. A.* **2009**, *106* (Suppl1), 9995−10000.

(56) Roberts, S. A.; Wildner, G. F.; Grass, G.; Weichsel, A.; Ambrus, A.; Rensing, C.; Montfort, W. R. *J. Biol. Chem.* **2003**, *278*, 31958−31963.

(57) Bloom, J. D.; Labthavikul, S. T.; Otey, C. R.; Arnold, F. H. *Proc. Natl. Acad. Sci. U. S. A.* **2006**, *103*, 5869−5874.